Nanoscale Res Lett (2010) 5:231–236
DOI 10.1007/s11671-009-9470-z

NANO EXPRESS

Hierarchical Cd_4SiS_6/SiO_2 Heterostructure Nanowire Arrays

Jian Liu · Chunrui Wang · Qingqing Xie · Junsheng Cai · Jing Zhang

Received: 1 August 2009 / Accepted: 14 October 2009 / Published online: 29 October 2009

Abstract Novel hierarchical Cd_4SiS_6/SiO_2 based heterostructure nanowire arrays were fabricated on silicon substrates by a one-step thermal evaporation of CdS powder. The as-grown products were characterized using scanning electron microscopy, X-ray diffraction, and transmission electron microscopy. Studies reveal that a typical hierarchical Cd_4SiS_6/SiO_2 heterostructure nanowire is composed of a single crystalline Cd_4SiS_6 nanowire core sheathed with amorphous SiO_2 sheath. Furthermore, secondary nanostructures of SiO_2 nanowires are highly dense grown on the primary Cd_4SiS_6 core-SiO_2 sheath nanowires and formed hierarchical Cd_4SiS_6/SiO_2 based heterostructure nanowire arrays which stand vertically on silicon substrates. The possible growth mechanism of hierarchical Cd_4SiS_6/SiO_2 heterostructure nanowire arrays is proposed. The optical properties of hierarchical Cd_4SiS_6/SiO_2 heterostructure nanowire arrays are investigated using Raman and Photoluminescence spectroscopy.

Keywords Cd_4SiS_6/SiO_2 · Nanowire arrays · Thermal evaporation · Optical property

Introduction

One-dimensional (1D) nanostructures with modulated compositions have recently become of particular interest with respect to potential applications in nanoscale building blocks of future optoelectronic devices and systems [1–3]. Among them, core/shell(or sheath) nanostructure materials can prevent oxidation of semiconductor 1D nanostructures and thus forestall interference in the building blocks of complex nanoscale circuits [4, 5]. Therefore, core/shell(or sheath)structures, such as nanocables, have attracted recent research focused on nanodevice applications such as field-effect transistors (FET) and light-emitting diodes (LED) [6, 7]. Very recently, significant progress has been made on the synthesis of complex 1D core/shell(or sheath) nanostructures such as Zn/ZnS core/shell (or sheath) fibers [8], TiO_2/SiO_2 nanocables [9], ZnS/SiO_2 core/shell(or sheath)nanowires [10, 11], and ZnO/SiO_2 core/shell nanorods [12]. Among these reports, most SiO_2 based 1D core/sheath (or core/shell) nanostructures were synthesized via complicated methods, such as high-temperature thermal evaporation of mixed materials [11] or two-step process [12].

However, the extensive reports of 1D core/shell(or sheath)structure growth have revealed several challenges that remain before these tools may practically be applied to commercial or industrial needs [10]. The first challenge is how to fabricate long nanostructures that can be easily integrated and manipulated post-synthesis through simple methods. The second challenge is how to organize the long nanostructures in ordered or aligned patterns and in high densities. The third challenge is how to form SiO_2 protective layer which is coated on 1D semiconductor nanostructures forms core/shell structures in order to protect the active layer in nanoelectronic circuits and obtain the noteworthy properties of the corresponding nanodevices [13, 14].

Cd_4SiS_6, a wide band gap semiconductor ($E_g = 2.50$ eV at 300 K), is a potential material used in electroluminescent devices (ELD) as its emission of visible light. To

J. Liu · C. Wang (✉) · Q. Xie · J. Cai · J. Zhang
Department of Applied Physics and State Key Laboratory for Modification of Chemical Fibers and Polymer Materials, Donghua University, 2999 Renmin Rd. North, 201620 Songjiang District, Shanghai, People's Republic of China
e-mail: crwang@dhu.edu.cn

date, only few works have been successfully completed on Cd–Si–S system. For example, Odin et al. [15] have reported the cathodoluminescence property of Cd_4SiS_6 crystal. Zhan et al. [16] have documented the synthesis and microstructure of Cd_4SiS_6/Si composite nanowires. In this paper, we report on the fabrication, structure, and properties of hierarchical Cd_4SiS_6/SiO_2 heterostructure nanowire arrays via a simple one-step thermal evaporation of CdS powder. The present work may be a rational route for meeting the earlier mentioned three obstacles.

Experimental Details

The as-grown hierarchical Cd_4SiS_6/SiO_2 heterostructure nanowire arrays were synthesized using a high-temperature vacuum-tube furnace, as described in detail elsewhere [17]. Briefly, CdS powder (1.5 g) was placed on an alumina boat in the center region of a quartz tube. Silicon substrates that were covered with Au thin film were placed in downstream to collect the products in the quartz tube. The tube was then pumped down to a base pressure of $\sim 2\times10^{-2}$ Torr (1 Torr $\approx$ 133 Pa). Argon gas was introduced into the tube at a constant flow rate of 200 sccm. The total pressure was kept at 2×10^{-2} Torr during the experimental process. The furnace was maintained at 900 °C for two hours before it was cooled to room temperature. A large yield of light yellow product was deposited on the silicon substrates.

The morphology of the samples was examined by scanning electron microscopy (SEM, FEI SIRION 200). The crystallographic structures of the as-grown product were investigated by X-ray diffraction (XRD, RIGAKU D/Max-2550), transmission electron microscopy (TEM, JEOL JEM-2010, operated at 200 kV), and high-resolution TEM (HRTEM, JEOL JEM-2010F, operated at 200 kV) equipped with an energy dispersive X-ray spectrometer (EDS) The Raman spectrum was recorded on Raman spectrometer (NEXUS-670) with 514.5 nm radiations at room temperature. Photoluminescence spectroscopy was performed using the Xe lamp spectrophotometer (970CRT) at 350-nm line.

Results and Discussions

SEM was used to examine the morphologies of the as-product. Figure 1a is a SEM image of the as-synthesized product. All the products display a wire-like (or rod-like) morphology with an average diameter ranging from 500 nm to 1 μm and length up to several millimeters. The sub-microwires (or sub-microrods) are well-aligned on silicon (100) substrates. The sub-microwires (or sub-microrods) grown mainly along two intersectant directions (indicated by arrows, as shown in Fig. 1a) which is similar to the case of ZnSe nanowires growth along <111> direction on GaAs (001) substrate [18] and Si, Ge nanowires growth along <111> direction on Si (001) substrate [19, 20], and the light–dark-light contrast was observed obviously along the wire's radial direction, which suggests the sub-microwire (or sub-microrod) with core/shell structure. XRD pattern of the as-grown products is shown in Fig. 1b. All the peaks can be indexed to monoclinic Cd_4SiS_6 structure with lattice constants $a = 12.31$ Å, $b = 7.041$ Å, $c = 12.33$ Å, $\beta = 110.38°$ (JCPDS Card. No. 72–0799). No peaks due to other phases such as CdS, Cd, and Si were detected, indicating the high purity of the products.

The detailed microstructures of Cd_4SiS_6 sub-microwires are characterized using TEM and HRTEM. Figure 2a is a typical TEM image of a single Cd_4SiS_6 sub-microwire from the as-grown product. The light–dark-light contrast was observed along the radial direction, suggesting different phase compositions with core/sheath structure along the wire's radial direction, which is in accord with the result of SEM. The diameter of the sub-microwire is

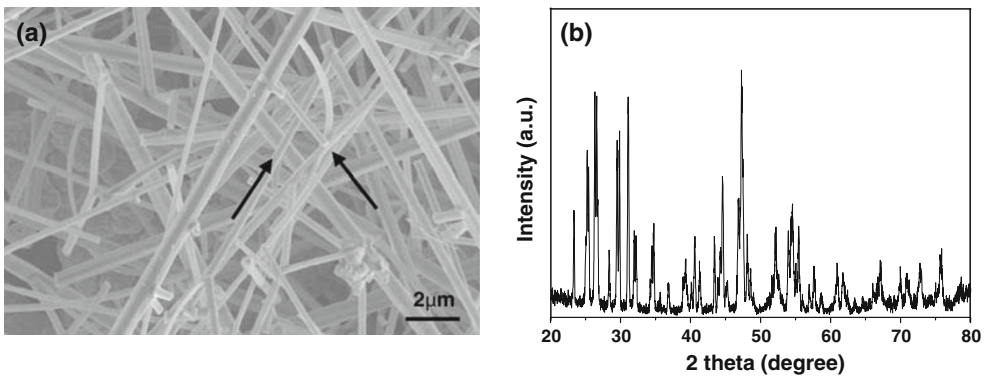

Fig. 1 **a** SEM image of the as-fabricated aligned sub-microwires, the arrows are the schematic directions of the sub-microwires. **b** The XRD pattern of the products

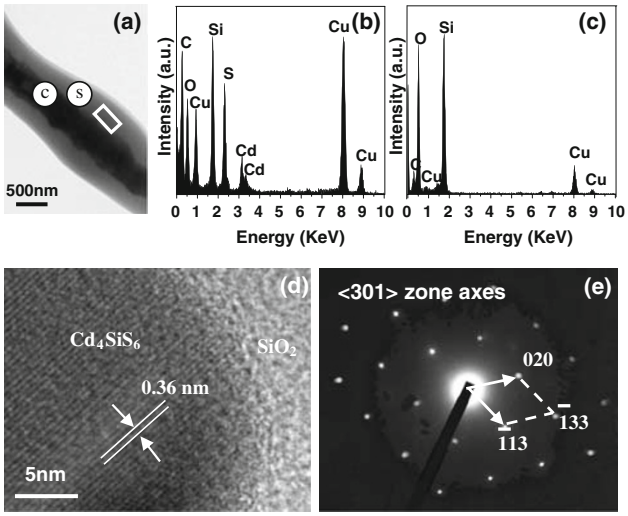

Fig. 2 **a** TEM image of single core/shell sub-microwire. **b**, **c** EDX patterns of the Cd_4SiS_6/SiO_2 core/shell sub-microwires' core and shell. **d** HRTEM image depicting the Cd_4SiS_6/SiO_2 core/shell sub-microwire. **e** SAED pattern of the Cd_4SiS_6/SiO_2 core/shell sub-microwire

approximately 1 μm, which also is consistent with SEM result. The diameter of the core and thickness of the sheath are approximately 300–500 nm and 250 nm, respectively. The compositions of the core and the shell of sub-microwire are checked using energy dispersive X-ray analysis (EDX), as shown in Fig. 2b–b indicates that the wire's core (marked as c, see Fig. 2a) is mainly composed of Cd, S, Si ,and O. EDX spectrum taken from the sub-microwire sheath (marked as s, as shown in Fig. 2a) shows the presence of Si and O with an approximate stoichiometry of SiO_2 (Fig. 2c). The peaks of Cu in those figures originate from the TEM sample grid. The EDX results clearly reveal the formation of Cd_4SiS_6 sub-microwires with SiO_2 sheath. The high-resolution TEM (HRTEM) image recorded from the joint part (as boxed region in Fig. 2a) of the core Cd_4SiS_6 and the shell SiO_2 is shown in Fig. 2d, which shows that the SiO_2 shells are amorphous, while the Cd_4SiS_6 core sub-microwires are single crystalline. The observed inter-planar d spacing is 0.36 nm corresponds well with that of the lattice spacing of $(\bar{1}33)$ planes of the Cd_4SiS_6. And it indicates that the Cd_4SiS_6 cores grow along the $[\bar{1}33]$ directions. The selected area electron diffraction (SAED) pattern is given in Fig. 2e, which further reveals that the Cd_4SiS_6 core has a single crystal structure. All studies reveal that the as-grown product is sub-microwires composited of single crystalline Cd_4SiS_6 core/amorphous SiO_2 sheath with uniform oriented wire-like morphologies.

Based on the earlier mentioned experimental result, we conducted the experiment with different parameters, that is, changed the position of silicon substrate, but kept the other parameters identical. And we obtained hierarchical of Cd_4SiS_6/SiO_2 heterostructure nanowire arrays.

Figure 3 is SEM images of as-synthesized hierarchical Cd_4SiS_6/SiO_2 nanowire arrays deposited on a silicon substrate after modifying the experimental parameters. Compared to the sample discussed earlier, although their XRD result is similar, their morphology differs tremendously. Figure 3a is a SEM image of the as-grown Cd_4SiS_6/SiO_2 hierarchical nanowires arrays on silicon substrate. The image reveals that the substrate is primarily covered with well-aligned hierarchical nanowires, which have an average diameter of 5 μm and length of several millimeters. The wires are rather uniform and grow vertically on silicon substrates. As shown in Fig. 3b, each wire has a cereus-like morphology, that is, there are uniform symmetrical secondary nanowires grown perpendicularly out of single nanowire. The secondary nanowires taper to tip and have length range from 1 to 2 μm as shown in Fig. 3c.

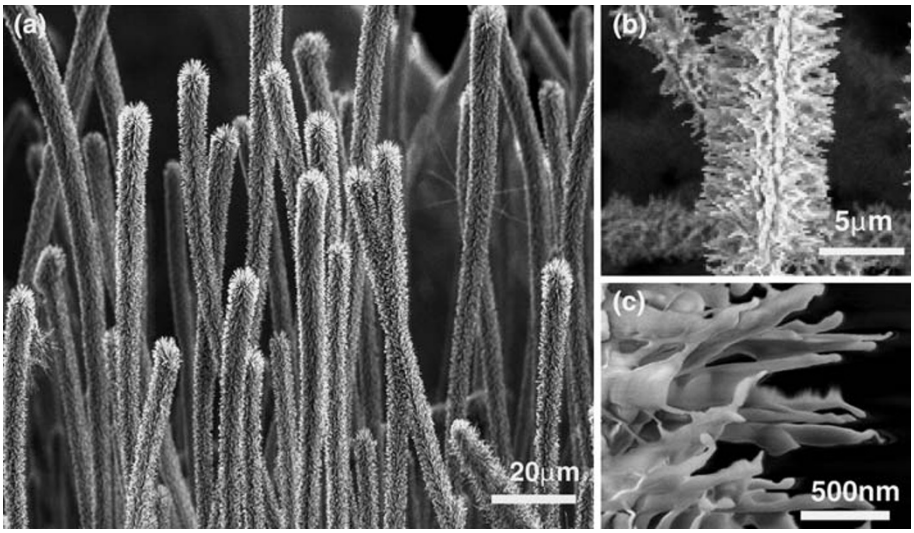

Fig. 3 **a** SEM image of the hierarchical nanowire arrays. **b** SEM of the single hierarchical nanowire. **c** SEM of the secondary nanowires

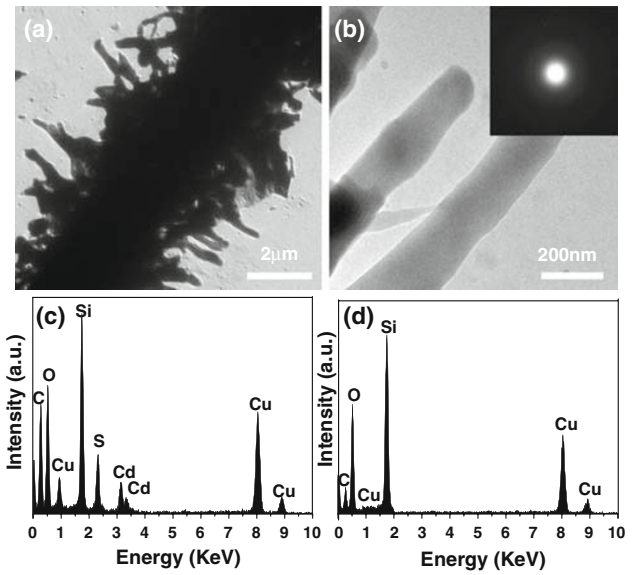

Fig. 4 **a** TEM image depicting single hierarchical nanowire. **b** TEM image of the secondary nanowires, insert is SAED of secondary nanowires. **c**, **d** EDX patterns of the Cd_4SiS_6/SiO_2 sub-microrods' body and secondary nanowires

The structures and morphologies of the hierarchical Cd_4SiS_6/SiO_2 nanowires were further characterized using TEM. Figure 4a is a TEM image of individual wire that presents a hierarchical morphology. The sub-microwire is uniform, with diameter of 5 μm. Figure 4b is the TEM image of the secondary nanowires, which shows the secondary nanowires are amorphous, with the diameter gradually decreasing from 200 to 100 nm. The insert in Fig. 4b is the SAED pattern of secondary nanowires, further confirms the secondary nanowires are amorphous. EDX of the body and the secondary nanowires are shown in Fig. 4c, d, which indicate that the sub-microwire's body is mainly composed of Cd, S, Si, O, and Cu, while the secondary nanowires are mainly composed of Si, O, and Cu. The peaks of Cu in these figures originate from the TEM sample grid. The TEM and EDX results demonstrate that the as-grown product is a composite material of Cd_4SiS_6/SiO_2 with hierarchical wire-like morphology.

The experimental results suggest that the hierarchical Cd_4SiS_6/SiO_2 heterostructure nanowires arrays are grown via a secondary growth mechanism. Based on thermodynamics [16], the chemical reactions involved in the process may be proposed as follows:

$$CdS(s) \rightarrow CdS(g) \quad (1)$$

$$Si + CdS \rightarrow Cd(g) + SiS \quad (2)$$

$$SiS + CdS \rightarrow Cd_4SiS_6 \quad (3)$$

$$SiS + 2O_2 \rightarrow SiO_2 + SO_2(g) \quad (4)$$

Based on all the earlier mentioned reactions, we deduce the possible formation process of the hierarchical Cd_4SiS_6/SiO_2 heterostructure nanowires arrays as shown in Fig. 5. CdS powder is gradually turned into CdS vapor under high temperature, which can be transported to the downstream region with argon gas. The small Au–Si alloy droplets on substrates are energetically favored sites for the absorption of incoming CdS vapor and residuary O_2 in the tube. This process leads to the formation of Cd_4SiS_6/SiO_2 core/shell nanocables, which can be used as templates for the secondary deposition of the SiO_2, resulting in the formation of secondary SiO_2 nanowires, and finally, leads to the formation of hierarchical Cd_4SiS_6/SiO_2 heterostructure nanowires arrays. The similar vapor transfer and second growth mechanism have been reported in previous works, such as Zn/ZnS core/shell fibers [8], hierarchical ZnS/SiO_2 nanowire heterostructures [11], and ZnSe/Si bi-coaxial nanowire heterostructures [21].

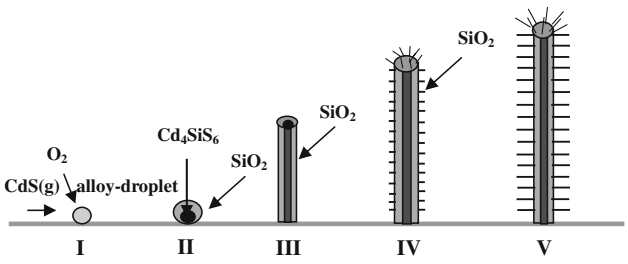

Fig. 5 Schematic illustration of the formation of hierarchical Cd_4SiS_6/SiO_2 nanowires via a secondary growth process. *I* formation of Au–Si alloy droplets, *II* simultaneous growth of Cd_4SiS_6 core and SiO_2 shell, *III* formation of $Cd_4SiS_6/SiO2$ sub-microcables, *IV*, *V* growth of hierarchical Cd_4SiS_6/SiO_2 nanowires

Figure 6a is structure model of monoclinic Cd_4SiS_6 crystal. In the monoclinic Cd_4SiS_6, both of silicon and cadmium atoms are surrounded by four sulfur atoms, and the SiS_4 tetrahedrons are interconnected by the CdS_4 tetrahedrons [16]. Therefore, Raman spectrum of Cd_4SiS_6 crystal displays a complex behavior with two modes, which can be assigned to the vibrational modes of Cd–S and Si–S. This behavior is very similar to $SnS_{2-x}Se_x$ [22], $NiS_{2-x}Se_x$ [23], and $PbSnS_3$ [24], which can be assigned to the vibrational modes of SnS_2 and $SnSe_2$, NiS_2 and $NiSe_2$, PbS and SnS_2, respectively. Figure 6b shows Raman spectrum of as-prepared hierarchical Cd_4SiS_6/SiO_2 nanowires arrays at room temperature. As far as we know, the spectrum of Cd_4SiS_6 structures has not been reported before in the literature. There are five Raman peaks at 209, 235, 302, 414, and 596 cm^{-1} in Fig. 6b. According to ref. [25], we can assign the most intensive peak at 414 cm^{-1} to the mode of $A_1(SiS_4)$. The peak at 302 and 596 cm^{-1} are attributed to the scatterings of the 1LO phonon (first order) and 2LO phonon (second order) of CdS, respectively, which has small blue-shift compared with that of the bulk CdS powders [26]. The small blue-shift might be caused by the

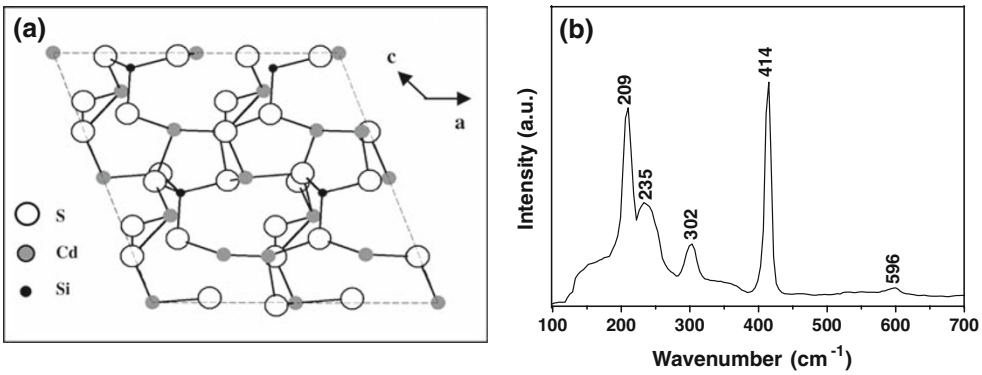

Fig. 6 **a** Structure model of Cd_4SiS_6 crystal. **b** Room-temperature Raman Spectrum of hierarchical Cd_4SiS_6/SiO_2 heterostructure nanowires

strong internal strain in the core [27]. The other two peaks at 209 and 235 cm^{-1} can be attributed to the scattering of the phonons of the CdS, which is consistent with previous reports of the CdS nanowires [26]. The multiphonon scatting and E_1-TO Raman bands of bulk CdS are located at 207 and 235 cm^{-1}, respectively [28]. Generally, the relative intensity of the vibtational mode of amorphous SiO_2 (frequencies at $\sim$1050 and $\sim$400 cm^{-1}, respectively) is too weak to be detected. In our research, although the thickness of amorphous SiO_2 sheath is comparable with the diameter of Cd_4SiS_6, Raman band of amorphous SiO_2 shell was not observed, which is similar to our previous report on the SiO_2 nanobelts [29].

Figure 7 shows the room-temperature PL properties of the as-grown hierarchical Cd_4SiS_6/SiO_2 heterostructure nanowires arrays. The spectrum shows two emission bands centered at 483 and 697 nm, respectively. The strong band located at 483 nm, which has been observed in a similar position in the CL spectra of Cd_4SiS_6 crystal [15], presumably results from near-band-edge emission of Cd_4SiS_6 cores ($E_g = 2.50$ eV). And the wide peak centered at 697 nm may be connected with the special core/sheath complex structures.

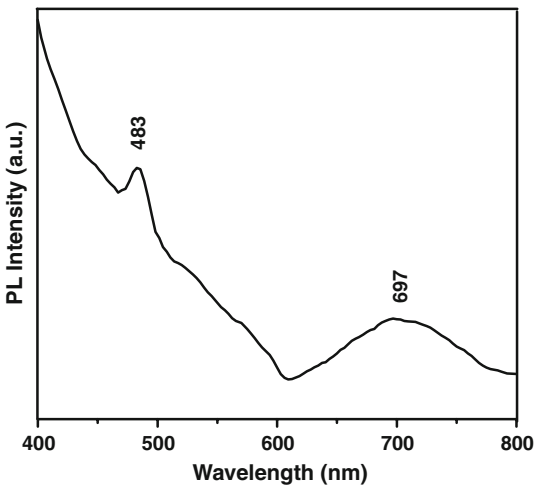

Fig. 7 Room-temperature PL Spectrum of hierarchical Cd_4SiS_6/SiO_2 heterostructure nanowires

Conclusions

In summary, hierarchical Cd_4SiS_6/SiO_2 heterostructure nanowires arrays have been prepared on silicon substrates via simple thermal evaporation with CdS powder. Studies indicate that the hierarchical Cd_4SiS_6/SiO_2 nanowires heterostructure arrays consist of a single crystalline Cd_4SiS_6 core coated amorphous SiO_2 and adjacent amorphous SiO_2 nanowires. The formation process of the hierarchical nanowires arrays was also discussed on the basis of thermodynamic aspect. The properties of hierarchical Cd_4SiS_6/SiO_2 heterostructure nanowires were characterized by RS and PL. The Raman peaks can be assigned to the modes of Cd–S and Si–S. In PL spectra, the peak at 483 nm can be identified as the near-band-edge emission of Cd_4SiS_6 cores. The long and uniform Cd_4SiS_6/SiO_2 heterostructure nanowires arrays may be applied as potential building blocks in nanodevices.

Acknowledgments This work was supported by the National Natural Science Foundation of China under Grant No. 20671018, 10775031, and 10835004.

References

1. Z.Y. Wang, B.B. Huang, Y. Dai, X.Y. Qin, X.Y. Zhang, P. Wang, H.X. Liu, J.X. Yu, J. Phys. Chem. C **113**, 4612 (2009)
2. M.S. Gudiksen, L.J. Lauhon, J. Wang, D.C. Smith, C.M. Lieber, Nature **415**, 617 (2002)
3. G.Z. Shen, D. Chen, C.W. Zhou, Chem. Mater. **20**, 3788 (2008)
4. J. Xu, X.L. Li, J.F. Liu, X. Wang, Q. Peng, Y.D. Li, J. Polym. Sci. A **43**, 2892 (2005)
5. J.H. He, Y.Y. Zhang, J. Liu, D. Moore, G. Bao, Z.L. Wang, J. Phys. Chem. C **33**, 12152 (2007)
6. F. Qian, S. Gradecak, Y. Li, C.Y. Wen, C.M. Lieber, Nano Lett. **5**, 2287 (2005)
7. J. Xiang, W. Lu, Y.J. Hu, Y. Wu, H. Yan, C.M. Lieber, Nature **441**, 489 (2006)

8. G.Z. Shen, D. Chen, C.J. Lee, J. Phys. Chem. C **111**, 5673 (2007)
9. J.M. Wu, J. Phys. Chem. C **112**, 13192 (2008)
10. D. Moore, J.R. Morber, R.L. Snyder, Z.L. Wang, J. Phys. Chem. C **112**, 2895 (2008)
11. G.Z. Shen, Y. Bando, C.C. Tang, D. Golberg, J. Phys. Chem. B **110**, 7199 (2006)
12. J.W. Zhao, L.Z. Wu, J.F. Zhi, J. Mater. Chem. **18**, 2459 (2008)
13. L. Liao, J.C. Li, D.F. Wang, C. Liu, C.S. Liu, Q. Fu, L.X. Fan, Nanotechnology **16**, 985 (2005)
14. C.X. Zou, X.Z. Zhang, G.Y. Jing, J.M. Zhang, Z.M. Liao, D.P. Yu, Appl. Phys. Lett. **92**, 253102 (2008)
15. I.N. Odin, M.V. Chukichev, V.A. Ivanov, M.E. Rubina, Inorg. Mater. **37**, 445 (2001)
16. J.H. Zhan, Y. Bando, J.Q. Hu, D. Golberg, J. Elect. Micro. **54**, 485 (2005)
17. C.R. Wang, J.M. Hou, J.O. Hou, Q. Li, Jpn. J. Appl. Phys. **43**, 7798 (2004)
18. Y. Cai, S.K. Chan, I.K. Sou, Y.F. Chan, D.S. Su, N. Wang, Small **3**, 111 (2007)
19. H. Adhikari, A.F. Marshall, C.E.D. Chidsey, P.C. McIntyre, Nano Lett. **6**, 318 (2006)
20. H.T. Ng, B. Chen, J. Li, J. Han, M. Meyyappan, Appl. Phys. Lett. **82**, 2023 (2003)
21. C.R. Wang, J. Wang, Q. Li, G.C. Yi, Adv. Funct. Mater. **15**, 1471 (2005)
22. S. Jandl, J.Y. Harbec, C. Carlone, Solid State Commun. **27**, 1441 (1978)
23. C. de las Heras, F. AgullÓ-Rueda, J. Phys. Condens. Mater **12**, 5317 (2000)
24. C.R. Wang, K.B. Tang, Q. Yang, G.Z. Shen, B. Hai, C.H. An, J. Zuo, Y.T. Qian, J. Solid State Chem. **160**, 50 (2001)
25. M. Ishii, M. Onoda, K. Shibata, Solid State Ionics. **121**, 11 (1999)
26. X.L. Fu, L.H. Li, W.H. Tang, Solid State Commun. **138**, 139 (2006)
27. D. Nesheva, C. Raptis, Phys. Rev. B **58**, 7913 (1998)
28. B. Tell, T.C. Damen, S.P.S. Porto, Phys. Rev. **144**, 771 (1966)
29. J. Liu, C.R. Wang, G.P. Ren, J. Wang, X.F. Xu, The Open Nanoscience Journal **2**, 43 (2008)